

# Mutations in the seed region of human miR-96 are responsible for nonsyndromic progressive hearing loss

Ángeles Mencía<sup>1,2</sup>, Silvia Modamio-Høybjør<sup>1,2</sup>, Nick Redshaw<sup>3</sup>, Matías Morín<sup>1,2</sup>, Fernando Mayo-Merino<sup>1,2</sup>, Leticia Olavarrieta<sup>1,2</sup>, Luis A Aguirre<sup>1,2</sup>, Ignacio del Castillo<sup>1,2</sup>, Karen P Steel<sup>4</sup>, Tamas Dalmay<sup>3</sup>, Felipe Moreno<sup>1,2</sup> & Miguel Ángel Moreno-Pelayo<sup>1,2</sup>

**MicroRNAs (miRNAs) bind to complementary sites in their target mRNAs to mediate post-transcriptional repression<sup>1,2</sup>, with the specificity of target recognition being crucially dependent on the miRNA seed region<sup>3</sup>. Impaired miRNA target binding resulting from SNPs within mRNA target sites has been shown to lead to pathologies associated with dysregulated gene expression<sup>4-7</sup>. However, no pathogenic mutations within the mature sequence of a miRNA have been reported so far. Here we show that point mutations in the seed region of miR-96, a miRNA expressed in hair cells of the inner ear<sup>8</sup>, result in autosomal dominant, progressive hearing loss. This is the first study implicating a miRNA in a mendelian disorder. The identified mutations have a strong impact on miR-96 biogenesis and result in a significant reduction of mRNA targeting. We propose that these mutations alter the regulatory role of miR-96 in maintaining gene expression profiles in hair cells required for their normal function.**

Nonsyndromic hearing impairment, with hearing loss as the only clinical feature, is a very frequent hereditary disorder characterized by high genetic and clinical heterogeneity. Some estimates predict that mutations in over 100 genes could be associated with this sensory deficit in humans. This extremely high genetic heterogeneity is a natural consequence of the anatomical and functional complexity of the ear. At present, around 100 loci for nonsyndromic hearing loss have been mapped, and in about half of them, the responsible genes, which encode a variety of proteins with very different functional roles, have been identified (see URLs section below). However, for a large number of mapped loci, the responsible genes remain to be identified.

We previously reported mapping of an autosomal dominant deafness locus (*DFNA50*) on 7q32 by studying a Spanish family (family 1) with postlingual, progressive, nonsyndromic all-frequency hearing loss<sup>9</sup> (Fig. 1a). Sequence analysis excluded *UBE2H*, *SMO*, *ATP6V1F*, *CALU*, *CCDC136*, *TSPAN33*, *KLHDC10*, *C7ORF68*, *FLNC*, *IMPDH1* and *MIR129-1* as genes responsible for *DFNA50* deafness. Subsequently, a set of three genes encoding miRNAs (*MIR96*, *MIR182*

and *MIR183*) was annotated within the interval. These genes are transcribed as a single polycistronic transcript and were reported to be expressed in the inner ear<sup>8</sup>; therefore, we considered them as candidate genes for *DFNA50* hearing loss. Sequencing of *MIR182* and *MIR183* in the proband (III:8) of family 1 did not reveal any changes in the entire precursor sequence. However, we found a G-to-A transition at position 13 in one allele of *MIR96*, miR96(+13 G>A), which replaced the fourth nucleotide within the conserved 7-nt seed region of the mature sequence (Fig. 1b). This mutation segregated with the hearing impairment in the family and was not detected in 462 unrelated normal-hearing Spanish controls. These findings implicate this mutation in *MIR96* as the cause of *DFNA50* hearing loss in this family.

Next, we extended the mutation screening of *MIR96* to our cohort of 567 genetically undiagnosed Spanish families with nonsyndromic sensorineural hearing loss: 238 of these had autosomal dominant hearing impairment, 84 showed autosomal recessive deafness, and in the remaining 245, the pattern of inheritance could not be defined unambiguously. We evaluated a proband from each family by dHPLC for the presence of heteroduplex in PCR products obtained by amplification of the *MIR96* genomic sequence. Sixteen samples resulted in dHPLC heteroduplexes, and subsequent sequence analysis identified three nucleotide substitutions. Two of them, miR96(+36T>C) and miR96(+42C>T), were located in the hairpin of the precursor sequence and were found in probands of four and ten different families, respectively; however, they did not segregate with the hearing loss in those families. Indeed, miR96(+36T>C) had been previously reported as a SNP (rs41274239). The last variant identified, miR96(+14 C>A), replaced the fifth nucleotide of the conserved seed region, just one base downstream of the position mutated in miR96(+13G>A) (Fig. 1b). This change was identified in the proband (III:1) of a family (family 2) with autosomal dominant, progressive, high-frequency hearing loss (Fig. 1a,c). We confirmed segregation of the mutation with the hearing loss in family 2; the mutation was not found in 462 normal-hearing Spanish controls.

We also carried out mutation screening of *MIR182* and *MIR183* in the same cohort of probands that we tested for *MIR96*. We detected a

<sup>1</sup>Unidad de Genética Molecular, Hospital Ramón y Cajal, Madrid, Spain. <sup>2</sup>Centro de Investigación Biomédica en Red de Enfermedades Raras (CIBERER), ISCIII, Madrid, Spain. <sup>3</sup>School of Biological Sciences, University of East Anglia, Norwich, UK. <sup>4</sup>Wellcome Trust Sanger Institute, Hinxton, Cambridge, UK. Correspondence should be addressed to M.A.M.-P. (mmoreno.hrc@salud.madrid.org).

G-to-A transition at position 106 of *MIR182* (located outside the mature sequence) in probands from 22 families, but it did not segregate with the hearing loss in any of them. We did not find any mutations in *MIR183*.

Alignment of the different pre-miR96 sequences from vertebrate species annotated in miRBase<sup>10</sup> (Fig. 2) revealed that nucleotides within the seed region at the contiguous positions +13 and +14 are among those fully conserved throughout vertebrate evolution, from

fish through primates, suggesting that they are crucial for the specific recognition of its target mRNAs (Fig. 2c). We used the Mfold program<sup>11</sup> to examine how these mutations could alter the predicted RNA secondary structure of pre-miR96. Both mutations introduce a base-pairing mismatch, decrease free energy values and create an enlarged RNA bulge in the predicted structure (Fig. 2a). In contrast, they do not seem to affect the ssRNA-dsRNA junction and the adjacent ~11-bp stem that are critical for the processing of pri-miRNA by the

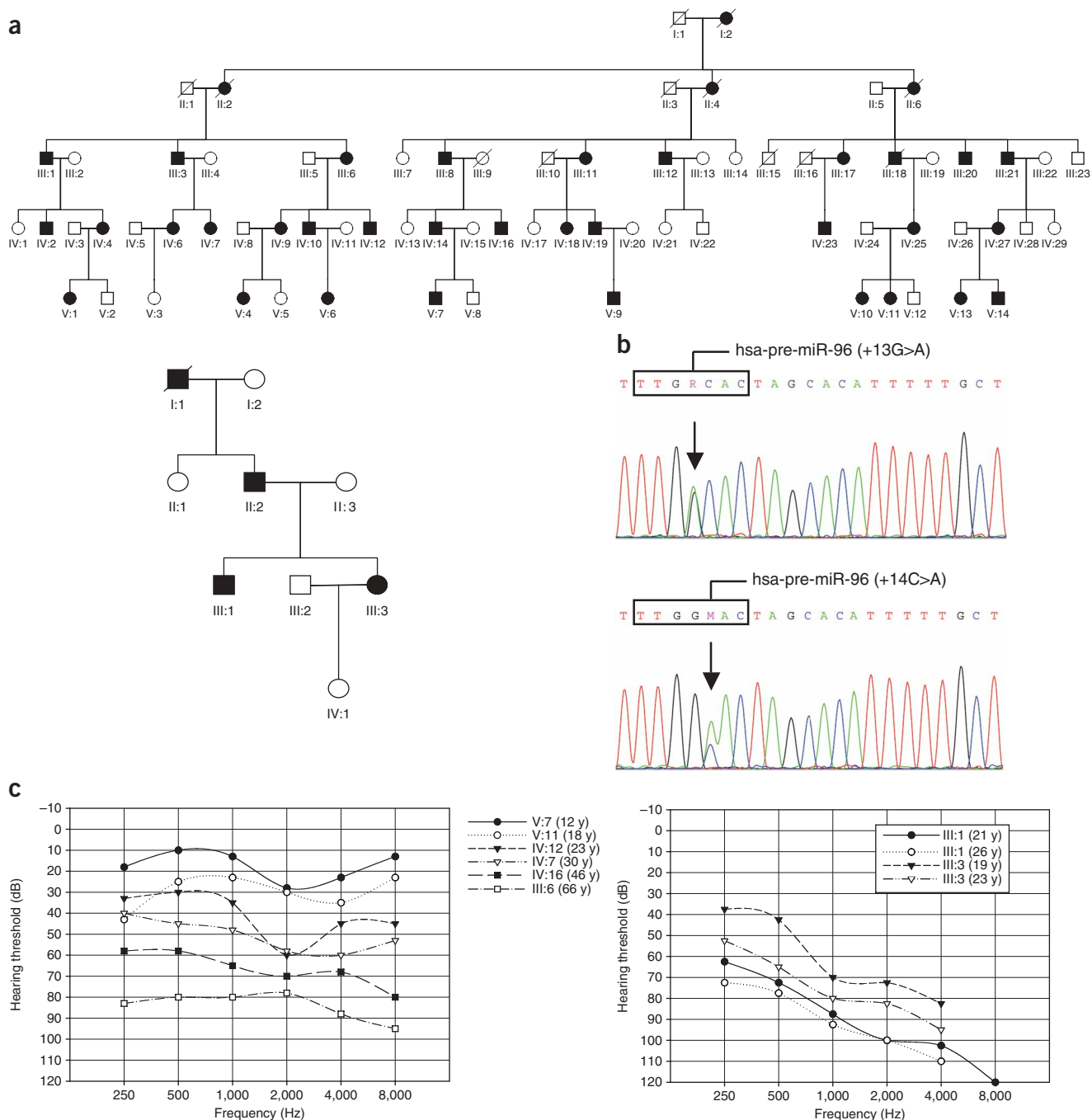
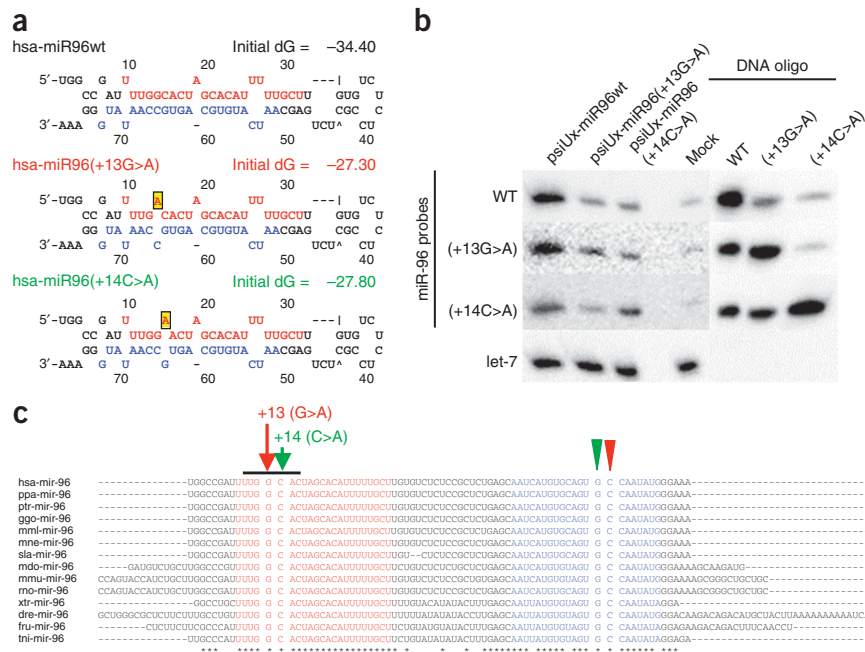


**Figure 1** Mutations in the seed region of *MIR96* cause *DFNA50* hearing loss. **(a)** Pedigrees of the Spanish families (family 1, top; family 2, bottom) segregating *DFNA50* hearing loss. Affected subjects are denoted in black. **(b)** Electropherograms depict the 23-nt mature sequence of human miR-96. The nucleotides corresponding to the seed region are boxed. The arrow points to the precise nucleotide that is mutated in each case. **(c)** Audiograms show the air conduction values obtained from different affected subjects of family 1 (left) and family 2 (right). The age of the subjects at which each audiometric record was obtained is indicated. Each graph point represents the average hearing loss for the right and left ears.

**Figure 2** Predicted secondary structure and processing of the wild-type and mutant forms of miR96. **(a)** Secondary structures of the wild-type and mutant pre-miR96 molecules as predicted by Mfold<sup>11</sup>. The miR-96 mature sequence is highlighted in red and the opposite strand (miR-96\*) in blue. The +13G>A and +14C>A mutations are shadowed in yellow. Free energies calculated by Mfold are indicated. **(b)** Mutations in miR-96 affect miRNA processing. Accumulation of the 23-nt mature form of miR96 was measured by RNA blot in RNA extracted from HeLa cells transfected with the wild-type and mutant forms of pre-miR96 cloned into psiUx plasmid (left, lanes psiUx-miR96wt, psiUx-miR96+13G>A and psiUx-miR96+14C>A). DNA oligonucleotides with identical sequences to wild-type and mutant miR-96 mature forms were used as controls for the hybridization (right panel, lanes WT, +13G>A and +14C>A).

The membrane was hybridized with the LNA-containing oligonucleotide probe specific for wild-type miR96 (top row, WT), then washed and reprobbed consecutively with the miR-96 probes specific for the mutant variants (rows, +13G>A or +14C>A). Equal loading is shown by hybridization with a let-7 specific probe. Wild-type miR-96 shows the highest accumulation with all three probes (left lane, psiUx-miR96wt), in spite of the preferential affinity of the mutant probes to the mutant miR-96 sequences (right panel, major diagonal). Similar results were obtained in five independent experiments carried out with independent transfections, RNA extractions, RNA blots and hybridizations. In two of these experiments, we used the mutant probes first and found the same results. **(c)** Multiple alignment of pre-miR96 sequences among different vertebrate species. Nucleotides at positions +13 and +14 and their complementary bases in the opposite strand (arrowheads) within the human pre-miR96 are fully conserved among the different pre-miR96 sequences of vertebrate species annotated in miRBase<sup>10</sup>. hsa, *Homo sapiens*; ppa, *Pan paniscus*; ptr, *Pan troglodytes*; ego, *Gorilla gorilla*; mml, *Macaca mulatta*; mne, *Macaca nemestrina*; sla, *Saguinus labiatus*; mdo, *Monodelphis domestica*; mmu, *Mus musculus*; rno, *Rattus norvegicus*; xtr, *Xenopus tropicalis*; dre, *Danio rerio*; fru, *Fugu rubripes*; tni, *Tetraodon nigroviridis*.

Equal loading is shown by hybridization with a let-7 specific probe. Wild-type miR-96 shows the highest accumulation with all three probes (left lane, psiUx-miR96wt), in spite of the preferential affinity of the mutant probes to the mutant miR-96 sequences (right panel, major diagonal). Similar results were obtained in five independent experiments carried out with independent transfections, RNA extractions, RNA blots and hybridizations. In two of these experiments, we used the mutant probes first and found the same results. **(c)** Multiple alignment of pre-miR96 sequences among different vertebrate species. Nucleotides at positions +13 and +14 and their complementary bases in the opposite strand (arrowheads) within the human pre-miR96 are fully conserved among the different pre-miR96 sequences of vertebrate species annotated in miRBase<sup>10</sup>. hsa, *Homo sapiens*; ppa, *Pan paniscus*; ptr, *Pan troglodytes*; ego, *Gorilla gorilla*; mml, *Macaca mulatta*; mne, *Macaca nemestrina*; sla, *Saguinus labiatus*; mdo, *Monodelphis domestica*; mmu, *Mus musculus*; rno, *Rattus norvegicus*; xtr, *Xenopus tropicalis*; dre, *Danio rerio*; fru, *Fugu rubripes*; tni, *Tetraodon nigroviridis*.



Drosha-DGCR8 complex<sup>12</sup>. A recent study, however, described a SNP within the seed region of miR125a that alters its processing to the mature form<sup>13</sup>. To examine the potential impact of the mutations we detected on miR96 biogenesis, we investigated expression and maturation of miR96 by RNA blot analysis. We transfected HeLa cells with vectors designed to express genomic fragments, each one containing the predicted hairpin and flanking sequences of the wild-type and both miR96 mutant alleles, as previously described<sup>14</sup>. Although the expression of the 23-nt mature form was readily detected for each of the three constructs, we observed an 80% decrease in the level intensity of both mutants relative to the wild type. This finding suggests that both mutations impair, but do not abrogate, processing of miR96 to its mature form (Fig. 2b and Supplementary Fig. 1 online). As miR-96/182/183 is transcribed as a polycistronic unit, an additional indirect effect on the expression of miR-182 and miR-183 due to the miR-96 mutations remains a possibility.

Because the mutations are located in the seed region of miR-96, and measurable amounts of both mutants can be still detected, we investigated the effect that these mutations could have on mRNA targeting. First, we searched for potential direct targets predicted by bioinformatic programs (miRanda, TargetScan and PITA programs<sup>3,15-17</sup>) and assessed the gene-silencing capacities of both mutants in luciferase assays. The search parameters take into account the complementarity, evolutionary conservation and accessibility of target sites to miR-96. From the list of potential targets (> 700), we selected five genes (*AQP5*, *CELSR2*, *ODF2*, *MYRIP* and *RYK*; Supplementary Fig. 2 online) that contained binding sites with perfect match to the miR-96 seed region and that were expressed in the inner ear<sup>18</sup>. We co-transfected siRNAs designed to mimic the wild type and both mutants into NIH-3T3 cells

with a construct containing the luciferase reporter coupled to the 3' UTR of each gene (pGL3-3'UTR). This reporter system showed that the translational level of all five luciferase-UTR constructs was controlled by human miR-96, and that both mutations led to reduced silencing of luciferase expression compared to wild-type miR-96. In all assays except one (+14C>A on *CELSR2*), the lack of repression was statistically significant (Fig. 3b). We verified that the ability to down-regulate these five luciferase-UTR transcripts was impaired when the putative 3'UTR-binding sites were disrupted, thus confirming that the observed effects were specific to miR-96 acting on the cloned UTR sequences (Supplementary Fig. 3 online).

The second possibility we investigated was that the mutations led to the silencing of potential acquired targets, that is, those containing binding sites complementary to the mutant seed regions of miR-96. To examine this, we conducted a bioinformatic search (TargetScan) using each mutated seed region as a query. The first one (UUGACAC; +13 G>A) perfectly matched that of miR-514, suggesting that, among the miR-514 predicted targets expressed in the inner ear (~90, UniGene), some could be regulated by this mutant. The second one (UUGAAC, +14 C>A) did not match that of any known miRNAs; however, the computer analysis rendered over 150 potential targets expressed in the inner ear. For the two mutants, we selected a subset of potential acquired targets (*MYO1B*, *ZIC1*, *SEMA6D* and *COL2A1* for miR96(+13G>A) and *SLC19A2*, *TJP1*, *LMX1A*, *MYLK* and *FMNL2* for miR96(+14 C>A); Supplementary Figs. 4 and 5 online) and assessed the repression capacities in luciferase assays. In six of them, the luciferase activity was slightly decreased relative to levels with wild-type miR-96 when assayed with the corresponding mutant, but only two of them (*SEMA6D* and *SLC19A2*) showed borderline but

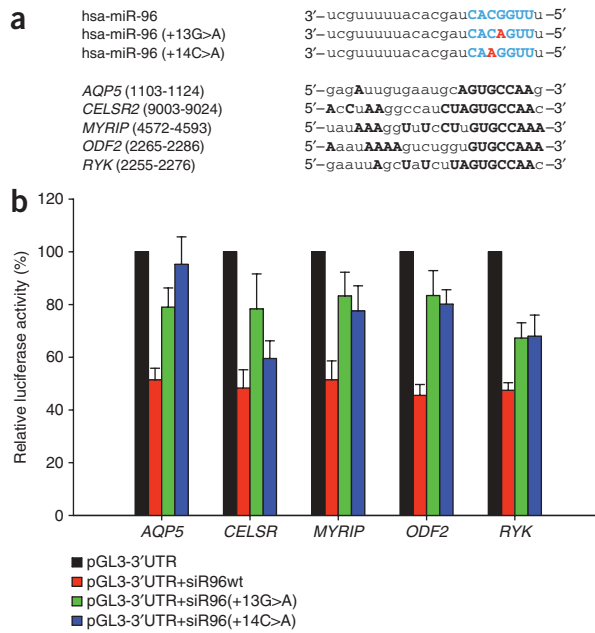


**Figure 3** Downregulation of predicted primary targets is impaired by the miR-96 (+13G>A) and (+14C>A) mutations. **(a)** Alignment of wild-type and mutant miR-96 mature sequences, and the putative binding sites within the 3'-UTR regions of the predicted direct targets. The exact positions of the sequence fragments of *AQP5*, *CELSR2*, *MYRIP*, *ODF2* and *RYK* transcripts are indicated. The nucleotides corresponding to the seed region of miR-96 are in blue, and the nucleotide mutated in each case in red. The matches within the binding sites with respect to the wild-type miR-96 sequence are indicated in boldface. **(b)** Luciferase reporter assay data from cells transfected with the pGL3 vector coupled to the 3'-UTR regions (pGL3-3'UTR) of the five predicted miR-96 primary targets indicated above. The five targets are downregulated by a siRNA designed to mimic miR-96 (siR96wt). Targeting was significantly impaired when siRNAs bearing each of the human mutations, siR96 (+13G>A) or siR96 (+14C>A), were used. Relative luciferase activity is expressed as mean  $\pm$  s.e.m. (four independent assays performed in triplicate for each target construct using at least two independent plasmid preparations) and normalized to the luciferase activity of the respective pGL3-3'UTR plasmids (black bars). *P* values for the difference between the luciferase activity obtained with siRwt (red bars) and with the mutant alleles were calculated using Student's paired *t*-test;  $\alpha = 0.05$  (*AQP5*: siR96(+13G>A) *P* = 0.000627, siR96(+14C>A) *P* = 0.000242; *CELSR2*: siR96(+13G>A) *P* = 0.002709, siR96(+14C>A) *P* = 0.106782; *MYRIP*: siR96(+13G>A) *P* = 0.000053, siR96(+14C>A) *P* = 0.004887; *ODF2*: siR96(+13G>A) *P* = 0.000205, siR96(+14C>A) *P* = 0.000024; *RYK*: siR96(+13G>A) *P* = 0.01425, siR96(+14C>A) *P* = 0.024288).

statistically significant differences ( $P = 0.04452$  and  $P = 0.039336$ , respectively) (Supplementary Fig. 6 online). This may indicate that, as a general trend, no significant gain of function is associated with these mutations, at least for the potential acquired targets investigated.

The set of three genes encoding miR-96, miR-182 and miR-183 comprises a sensory tissue-specific miRNA cluster with an exceptional conservation of expression in ciliated neurosensory organs among both vertebrate and invertebrate organisms<sup>8,19–22</sup>. The miR-183/96/182 cluster is detected in the hair cells of the cochlea and vestibule in the early postnatal mouse inner ear through to adulthood, with slight changes in expression levels, suggesting that these microRNAs are evolutionarily associated with mechanosensory cell specification and function<sup>8</sup>. As both miR-96 mutants behave similarly for the different direct targets tested in the luciferase assays (Fig. 3b), they will presumably share a wide range of targets that are dysregulated. The expected small variations in the subset of dysregulated targets as a consequence of those specifically acquired by each mutation could contribute to the subtle phenotypic differences observed in these two families (Fig. 1 and Supplementary Methods online). The fact that both families manifest the hearing loss postlingually indicates that neither mutation likely results in impaired development of the inner ear; instead, they could have an impact on the regulatory role that miR-96 plays in hair cells of the adult cochlea to maintain gene expression profiles required for its normal function.

In mouse retina, the miR-183/96/182 cluster is highly expressed in photoreceptors, bipolar and amacrine cells. As in the inner ear, these miRNAs may have important roles during the last steps of differentiation and function of the mature retina<sup>19</sup>. However, after ophthalmologic revision, we observed no ocular phenotype in individuals carrying mutations in miR-96 (age range between 2 and 66 years), suggesting that its specific targets in retina are not critical for its function or that the translation of these targets is not markedly affected.

Although deficiencies or excesses of miRNA expression are associated with the development and progression of a variety of human pathologies ranging from myocardial infarction to cancer<sup>23,24</sup>, this is the first study to show that nucleotide substitutions in the seed region of a miRNA are responsible for a human mendelian disease, in which

misprocessing of miR-96 and impaired miRNA-target recognition could be invoked as the most likely mechanism of pathogenesis. The finding of a different point mutation in the seed region of miR-96 in a mouse mutant with hair cell defects and progressive hearing loss, as described in the accompanying report<sup>18</sup>, further supports the proposal that the mutations we identified here are responsible for *DFNA50* hearing loss. Deciphering the different targets that are dysregulated by these mutations will shed light on the biological processes that are affected and should help to design specific therapies to palliate the progressive hearing deterioration in individuals carrying these mutations.

## METHODS

**Mutation screening and computational methods.** We designed primers pairs to amplify the precursor sequences of *MIR96*, *MIR182* and *MIR183* from genomic DNA (Supplementary Table 1 online). PCR was performed by standard procedures as previously described<sup>25</sup>. PCR amplicons were screened for mutations by DHPLC (denaturing high-performance liquid chromatography) on a Wave DNA fragment analysis system (Transgenomic), according to manufacturer's protocol and the different heteroduplex profiles characterized by automatic sequencing (Applied Biosystems). We used the Mfold program<sup>11</sup> to evaluate the possible impact on the secondary structure of pre-miR96 caused by the mutations. The target genes used in the luciferase assays were selected using miRanda, TargetScan, and PITA programs (see URLs section below).

**Analysis of function and biogenesis.** Luciferase reporters were constructed with 3' UTRs amplified from genomic DNA and cloned in pGL3 vector<sup>26</sup>. siRNAs were designed to mimic miR-96 (siR96), miR-96 containing the family 1 (siR96+13G>A) or family 2 (siR96+14C>A) mutations, and miR-140 (siR140) as a negative control (Supplementary Table 2 online). Positive-control constructs were made for each siRNA in which synthetic double-stranded oligonucleotides containing the complementary sequences to the mature miRNAs were cloned into the same position as the above target constructs. We carried out luciferase assays 24 h after transfection using the Luciferase Reporter Gene Assay kit (Roche). Luciferase activity was normalized to protein content measured using the BCA protein assay kit (Pierce). Relative reporter activity for siRNA-treated cells was obtained by normalization to the luciferase activity of the respective target constructs transfected alone. miRNA precursor and flanking sequences of wild-type miR-96 and both mutants (miR96(+13G>A) and miR96(+14C>A)) were amplified from genomic

DNA and cloned into the psiUx expression vector (**Supplementary Table 3** online)<sup>14</sup>. After transfection, total RNA was isolated using miRVana kit (Ambion), and blotted to Hybond NX (Amersham) membranes and linked with carbodiimide<sup>27</sup>. We detected the 23-nt mature sequences of wild-type miR-96 and both mutants using specific locked nucleic acid (LNA) probes in each case. The quantification of the band-intensity levels in the RNA blot was performed by the Kodak 1D 3.5 program (Scientific Imaging Systems), with the net intensity of the bands measured in arbitrary units (AU). Additional details are available in **Supplementary Methods**.

**URLs.** Hereditary hearing loss homepage, <http://webhost.ua.ac.be/hhh/>; miRanda v3.0, <http://www.microrna.org/microrna/home.do>; TargetScan v4.2, <http://www.targetscan.org/>; PITA, Probability of Interaction by Target Accessibility, <http://genie.weizmann.ac.il/pubs/mir07/>.

**Accession codes.** GenBank EntrezGene: *UBE2H*, 7328; *SMO*, 6608; *ATP6V1F*, 9296; *CALU*, 813; *CCDC136*, 64753; *TSPAN33*, 340348; *KLHDC10*, 23008; *HIG2*, 29923; *FLNC*, 2318; *IMPDH1*, 3614; *MIR129-1*, 406917; *AQP5*, 362; *CELSR2*, 1952; *ODF2*, 4957; *MYRIP*, 25924; *RYK*, 6259; *MYO1B*, 4430; *ZIC1*, 7545; *SEMA6D*, 80031; *COL2A1*, 1280; *SLC19A2*, 10560; *TJP1*, 7082; *LMX1A*, 4009; *MYLK*, 4638; *FMNL2*, 114793. GenBank EntrezNucleotide: *AQP5*, BC032946; *CELSR2*, NM\_001408; *MYRIP*, NM\_015460; *ODF2*, NM\_153437; *RYK*, NM\_001005861.

Note: Supplementary information is available on the Nature Genetics website.

#### ACKNOWLEDGMENTS

We thank members of the Spanish families whose participation made this study possible. We also express our gratitude to A. Fatica and I. Bozzoni (Universita di Roma "La Sapienza") for the donation of the microRNA expression vector and to P. Morales (Hospital 12 de Octubre) for providing control DNAs. S.M.-H. is recipient of a fellowship from L'Oréal-UNESCO "for women in Science". A.M. is recipient of a contract from the Centre for Biomedical Research on Rare Diseases (CIBERER) and M.M. is recipient of a contract from the EuroHear project. F.M.-M. is a fellow from the Spanish Ministerio de Ciencia y Tecnologia. This work was supported by grants from the Spanish Ministerio de Ciencia y Tecnologia (SAF2005-06355 to F.M.), Spanish Fondo de Investigaciones anitarias (FIS CP03/00014 and PI08/0045 to M.A.M.-P.; PI-051942; G03/203), the European Commission (FP6 Integrated Projects: SIROCCO LSHG-CT-2006-037900 to T.D.; EUROHEAR, LSHG-CT-2004-512063), Deafness Research UK and the Wellcome Trust.

#### AUTHOR CONTRIBUTIONS

The exclusion of candidate genes within the *DFNA50* genetic interval and the identification of the miR96 mutations were carried out by A.M., S.M.-H., M.M., F.M.-M. and L.O. Screening in autosomal recessive deafness families was designed and performed by I.d.C. and L.A.A. Vector generation for luciferase assays and miR96 expression was carried out by A.M., and the experiments were designed and performed by N.R. and T.D. Experimental design of the study and writing of the manuscript was carried out by M.A.M.-P. K.P.S. shared data and ideas. Scientific discussion of data and critical reading of the paper were performed by K.P.S., T.D., I.d.C., F.M. and M.A.M.-P.

Published online at <http://www.nature.com/naturegenetics/>

Reprints and permissions information is available online at <http://npg.nature.com/reprintsandpermissions/>

1. Kloosterman, W.P. & Plasterk, R.H. The diverse functions of microRNAs in animal development and disease. *Dev. Cell* **11**, 441–450 (2006).

2. He, L. & Hannon, G.J. MicroRNAs: small RNAs with a big role in gene regulation. *Nat. Rev. Genet.* **5**, 522–531 (2004).
3. Lewis, B.P., Burge, C.B. & Bartel, D.P. Conserved seed pairing, often flanked by adenosines, indicates that thousands of human genes are microRNA targets. *Cell* **120**, 15–20 (2005).
4. Abelson, J.F. *et al.* Sequence variants in *SLITRK1* are associated with Tourette's syndrome. *Science* **310**, 317–320 (2005).
5. Clop, A. *et al.* A mutation creating a potential illegitimate microRNA target site in the myostatin gene affects muscularity in sheep. *Nat. Genet.* **38**, 813–818 (2006).
6. Sethupathy, P. *et al.* Human microRNA-155 on chromosome 21 differentially interacts with its polymorphic target in the *AGTR1* 3' untranslated region: a mechanism for functional single-nucleotide polymorphisms related to phenotypes. *Am. J. Hum. Genet.* **81**, 405–413 (2007).
7. Jensen, K.P. *et al.* A common polymorphism in serotonin receptor 1B mRNA moderates regulation by miR-96 and associates with aggressive human behaviors. *Mol. Psychiatry* advance online publication, doi:10.1038/mp.2008.15 (19 February 2008).
8. Weston, M.D., Pierce, M.L., Rocha-Sanchez, S., Beisel, K.W. & Soukup, G.A. MicroRNA gene expression in the mouse inner ear. *Brain Res.* **1111**, 95–104 (2006).
9. Modamio-Højbyør, S. *et al.* A novel locus for autosomal dominant nonsyndromic hearing loss, DFNA50, maps to chromosome 7q32 between the DFN17 and DFN13 deafness loci. *J. Med. Genet.* **41**, e14 (2004).
10. Griffiths-Jones, S., Grocock, R.J., van Dongen, S., Bateman, A. & Enright, A.J. miRBase: microRNA sequences, targets and gene nomenclature. *Nucleic Acids Res.* **34**, D140–D144 (2006).
11. Zuker, M. Mfold web server for nucleic acid folding and hybridization prediction. *Nucleic Acids Res.* **31**, 3406–3415 (2003).
12. Han, J. *et al.* Molecular basis for the recognition of primary microRNAs by the Drosha-DGCR8 complex. *Cell* **125**, 887–901 (2006).
13. Duan, R., Pak, C. & Jin, P. Single nucleotide polymorphism associated with mature miR-125a alters the processing of pri-miRNA. *Hum. Mol. Genet.* **16**, 1124–1131 (2007).
14. Denti, M.A., Rosa, A., Sthandier, O., De Angelis, F.G. & Bozzoni, I. A new vector, based on the PolII promoter of the U1 snRNA gene, for the expression of siRNAs in mammalian cells. *Mol. Ther.* **10**, 191–199 (2004).
15. Enright, A. *et al.* MicroRNA targets in *Drosophila*. *Genome Biol.* **5**, R1 (2003).
16. John, B. *et al.* Human microRNA targets. *PLoS Biol.* **2**, 1862–1879 (2004).
17. Kertesz, M., Iovino, N., Unnerstall, U., Gaul, U. & Segal, E. The role of site accessibility in microRNA target recognition. *Nat. Genet.* **39**, 1278–1284 (2007).
18. Lewis, M. *et al.* An ENU-induced mutation of miR96 associated with progressive hearing loss in mice. *Nat. Genet.* advance online publication, doi:10.1038/ng.369 (12 April 2009).
19. Xu, S., Witmer, P.D., Lumayag, S., Kovacs, B. & Valle, D. MicroRNA (miRNA) transcriptome of mouse retina and identification of a sensory organ-specific miRNA cluster. *J. Biol. Chem.* **282**, 25053–25066 (2007).
20. Kloosterman, W.P., Wienholds, E., de Bruijn, E., Kauppinen, S. & Plasterk, R.H. *In situ* detection of miRNAs in animal embryos using LNA-modified oligonucleotide probes. *Nat. Methods* **3**, 27–29 (2006).
21. Wienholds, E. *et al.* MicroRNA expression in zebrafish embryonic development. *Science* **309**, 310–311 (2005).
22. Pierce, M.L. *et al.* MicroRNA-183 family conservation and ciliated neurosensory organ expression. *Evol. Dev.* **10**, 106–113 (2008).
23. Calin, G.A. *et al.* Frequent deletions and down-regulation of microRNA genes miR15 and miR16 at 13q14 in chronic lymphocytic leukemia. *Proc. Natl. Acad. Sci. USA* **99**, 15524–15529 (2002).
24. Soifer, H., Rossi, J.J. & Saetrom, P. MicroRNAs in disease and potential therapeutic applications. *Mol. Ther.* **15**, 2070–2079 (2007).
25. del Castillo, I. *et al.* A deletion involving the connexin 30 gene in nonsyndromic hearing impairment. *N. Engl. J. Med.* **346**, 243–249 (2002).
26. Tuddenham, L. *et al.* The cartilage specific microRNA-140 targets histone deacetylase 4 in mouse cells. *FEBS Lett.* **580**, 4214–4217 (2006).
27. Pall, G.S., Codony-Servat, C., Byrne, J., Ritchie, L. & Hamilton, A. Carbodiimide-mediated cross-linking of RNA to nylon membranes improves the detection of siRNA, miRNA and piRNA by northern blot. *Nucleic Acids Res.* **35**, e60 (2007).